

# Experimental study of the flow regime effect on the stability of collapsible tubes conveying fluid

Cite as: Phys. Fluids **33**, 064104 (2021); <https://doi.org/10.1063/5.0050745>

Submitted: 18 March 2021 . Accepted: 01 May 2021 . Published Online: 03 June 2021

 A. Podoprosvetova,  J. Zayko,  V. Yushutin, and  V. Vedenev



View Online



Export Citation



CrossMark

Physics of Fluids

**SPECIAL TOPIC:** Tribute to  
Frank M. White on his 88th Anniversary

SUBMIT TODAY!



# Experimental study of the flow regime effect on the stability of collapsible tubes conveying fluid

Cite as: Phys. Fluids **33**, 064104 (2021); doi: 10.1063/5.0050745

Submitted: 18 March 2021 · Accepted: 1 May 2021 ·

Published Online: 3 June 2021



View Online



Export Citation



CrossMark

A. Podoprosvetova,<sup>1,a)</sup>  J. Zayko,<sup>1</sup>  V. Yushutin,<sup>2</sup>  and V. Vedenev<sup>1</sup> 

## AFFILIATIONS

<sup>1</sup>Institute of Mechanics, Lomonosov Moscow State University, Moscow 119991, Russia

<sup>2</sup>Department of Mathematics, University of Maryland, College Park, Maryland 20742-4015, USA

<sup>a)</sup>Author to whom correspondence should be addressed: [podoprosvetova@imec.msu.ru](mailto:podoprosvetova@imec.msu.ru)

## ABSTRACT

Experimental studies of the stability of the collapsible tubes conveying fluid have been previously conducted in the context of cardiovascular mechanics mostly for turbulent flows, although blood flows are laminar under normal conditions. In this paper, the turbulent and laminar regimes with equal flow rates and pressure drops are investigated experimentally to identify the stability boundary and self-exciting oscillation modes of Penrose tubes conveying fluid in the Starling resistor. Four oscillation modes for laminar and for turbulent regimes were observed visually and by measuring the pressure drop and the output pressure. Comparison of amplitudes, frequencies, and boundaries between different oscillation modes for equivalent laminar and turbulent flow regimes is performed.

Published under an exclusive license by AIP Publishing. <https://doi.org/10.1063/5.0050745>

## I. INTRODUCTION

The interaction of the blood flow with vessels and the possible loss of stability in this hydroelastic system are important problems of cardiovascular mechanics. Several physiological examples of blood vessel collapse were discussed by Shapiro,<sup>1,2</sup> Kamm and Shapiro,<sup>3</sup> Pedley,<sup>4</sup> Pedley *et al.*,<sup>5</sup> Koshev *et al.*,<sup>6</sup> such as the collapse due to hydrostatic reduction of the transmural pressure, i.e., the difference between internal and external vessel pressures. We refer the interested reader to Grotberg and Jensen,<sup>7</sup> Bertram,<sup>8</sup> and Heil and Hazel<sup>9</sup> for an overview of theoretical and experimental studies of the collapsible tubes conveying fluid.

The one-dimensional model is the most common method for the theoretical study of the blood flow in vessels (Refs. 10–19). Although in many cases, it is sufficient to study integral properties of the “wall-fluid” system (e.g., Refs. 20 and 21) to analyze various instabilities, a number of authors use two-dimensional (Refs. 22–26) or three-dimensional models of the fluid flow through elastic tubes to get a more detailed description of the instability mechanisms (Refs. 27–30).

The classical experimental apparatus used to examine properties of blood vessel models is the Starling resistor (Ref. 31). The complex fluid-structure interaction during vibrations leads to various types of instabilities with low, intermediate, and high frequencies (Ref. 32) which result in a reduction of the flow rate and increase of the pressure drop.

Since vascular walls in biological systems are soft and deformable (Refs. 7, 33, and 34) it is convenient to utilize latex (silastic) rubber

and Penrose drainage tubes to model blood vessels as initially suggested by Gavriely *et al.*<sup>35</sup> and Brower and Noordergraaf,<sup>36</sup> respectively. Gavriely *et al.*<sup>35</sup> measured the pressure-flow relationships by gradually increasing the pressure drop along the tube. They observed loud honking sounds and oscillations of the tube that occur only when the flow rate becomes constant and independent of downstream driving pressure. Also, the oscillatory frequencies are higher at larger flow velocities and in the case of narrower distances between opposing flattened walls. Bertram and Castles<sup>37</sup> investigated the flow rate limitation of the thick-walled silicone-rubber tubes conveying water and it was found that the flow rate depends not only on the upstream transmural pressure but also on its history, in a hysteretic manner. Later, Bertram and Elliott<sup>38</sup> conducted experiments with thin-walled tubes to study the effect of wall thickness. As in a thick tube, there is a dramatic reduction of the flow rate when a collapse and the flow limitation start, but there is only a slight increase in the flow rate when the tube recovers the circular shape.

Wang *et al.*<sup>39</sup> identified the connection between the flow rate and its limitation and pressure  $P$  at the point of collapse initiation for various inner diameters, lengths, and thicknesses of the tube. Two flow limitation modes were found: in the first, the flexible tube retains a circular shape for  $P < P_a$  and it starts to oscillate at  $P \approx P_a$ ; in the second mode, the flexible tube also retains a circular shape at  $P < P_a$ , but it collapses in a static manner for  $P > P_a$  until the oscillations start at a higher pressure.

Most of these studies were conducted only for turbulent flows meaning that the flow rate limitation manifests when the fluid flow is not laminar anymore. Although turbulence does occur in stenotic vessels due to a strong increase in the linear velocity of blood flow, the presence of turbulence is limited to the ventricles of the heart, aortic ostium, and aortic arch, while the blood flow is laminar in other parts of the cardiovascular system. Consequently, a study of the effect of flow regime on the onset and character of oscillations of the model blood vessel is of great interest.

However, there are just a few studies on the effect of flow viscosity and flow regime on stability. Lyon *et al.*<sup>40</sup> studied the applicability of the theoretical waterfall model (Refs. 41 and 42) and the onset of oscillations in the Starling resistor for different fluid viscosities. The paper presented for the first time the pressure-flow relationships for a collapsible tube with low Reynolds number flow corresponding to laminar flows. Experiments showed that the pressure-flow relationships for low Reynolds number flows are distinctly different from those for moderate Reynolds number flows. The effect of fluid viscosity was also examined by Bertram and Tscherry.<sup>43</sup> They conducted experiments on collapsible tubes for laminar regimes with the lowest possible Reynolds numbers. The goal of that study was to provide experimental data for the validation of three-dimensional DNS codes, which are limited to sufficiently small Reynolds numbers. Zayko and Vedenev<sup>44</sup> experimentally studied the influence of flow regime on the limit cycle oscillations of latex thin-walled tube and showed that the oscillation frequency more essentially depends on the pressure drop in the tube for a fixed flow rate at laminar regimes, while the oscillation amplitude is larger for the turbulent regimes. However, in those experiments, the rigid tube before the collapsible segment was not sufficiently long to reach developed laminar or turbulent flow. A recent experimental study<sup>45</sup> investigates the effect of non-Newtonian fluid properties on steady flow in a collapsible tube.

It is seen from the literature review that there is some discrepancy between most of experimental studies with collapsible tubes, where the flow was turbulent, and biomechanical applications, where the flow is laminar. The aim of the present study is to highlight this gap and to analyze experimentally the effect of the fluid flow regime on the stability boundary and on the limit cycle oscillations of a thin-walled collapsible tube conveying fluid.

Let us consider the friction coefficient of a rigid tube as a function of Reynolds number (Fig. 1). It is seen that there is a range of laminar and turbulent regimes with equal friction coefficients. These regimes correspond to different Reynolds numbers and, for the same fluid, to different average velocities. Hence, dimensional pressure drops are not equal, which would lead to different shapes of an elastic tube. However, it is possible to take different fluids such that their Reynolds numbers will correspond to  $Re_l$  and  $Re_t$ , see Fig. 1, with equal pressure drops and the same average velocity. In result, these flows will be equivalent in their integral properties, and the only difference will be the regime, laminar, or turbulent. To organize such equivalent flows for a given flow rate, we use water and glycerin solutions that provide equal pressure drop and transmural pressure, which guarantees the similarity of the tube shapes. We then compare the results for the turbulent flow of water and the laminar flow of a glycerin solution in the same collapsible tube, which are equal in all integral parameters.

The paper is organized as follows: In Sec. II, we describe the apparatus used in experiments, calculate the glycerin concentration

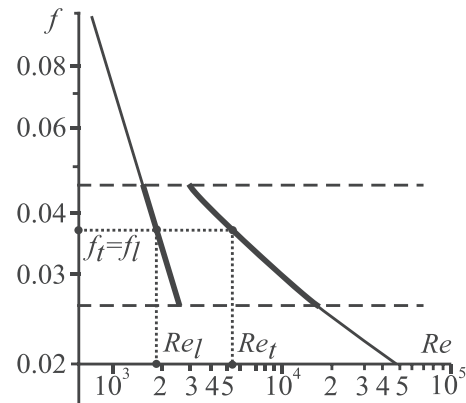


FIG. 1. Friction coefficient  $f$  of a flow in a rigid tube as a function of Reynolds number.

that yields integral flow characteristics equal to water flow, and analyze flow properties in an elastic tube. In Sec. III, we present the results of experiments, both for the stability boundary and for the characteristics of oscillations. Section IV is devoted to qualitative theoretical explanation and discussion of observed results. Finally, Sec. V summarizes the results and concludes the paper.

## II. EXPERIMENTAL METHODS AND PROCEDURES

### A. Experimental apparatus

The experimental study was conducted on the installation for the recirculation of fluid through the elastic tube shown in Fig. 2. The apparatus consists of a thin-walled Penrose tube that is mounted between two rigid tubes of the same diameter and placed in the chamber, of a drain and a base tanks, a pump, a flowmeter, differential pressure sensors, and two cameras. External pressure  $p_e$  in the chamber is constant. The tube with the unstretched diameter of 10 mm (as specified by the manufacturer; the actual value will be provided in Sec. II E), wall thickness of  $0.3 \pm 0.02$  mm, Young's modulus of 1.13 MPa and with the length of 0.44 m is stretched axially by 16%. Tube samples were regularly changed: either each 45 min of continuous operation, or after each change of the working fluid. In all regimes, experimental results were not affected by a particular tube specimen. The chamber, whose dimensions are  $100 \times 40 \times 50$  cm (length, height, and width), is made of glass and is filled with water to prevent sagging of the tube. The pump is controlled automatically by the fluid level sensor in the drain tank.

The inlet section consists of a tap shown in Fig. 2, followed by a rigid tube with 15 mm diameter and 0.5 m length; next, garden hose of 17.5 mm diameter and 2 m length that connects the first rigid tube with the next one, of 15 mm diameter and 1 m length; next, a smooth confuser,  $\sim 0.1$  m in length, which decreases radius from 15 to 10 mm, followed by a rigid tube of 10 mm diameter (the same as of an elastic tube) of 1 m length. This system of tubes provides developed laminar and turbulent flows in all experiments conducted: the hydrodynamic entrance length was not exceeding 1 m for laminar and 0.19 m for turbulent flows in all studied regimes. The rigid outlet section consists of a rigid tube of the same diameter as the elastic tube of 0.4 m length, a smooth diffuser, a rigid tube of 15 mm diameter and 0.35 m length, and a garden drain hose of 17.5 mm diameter and 5 m length. Both

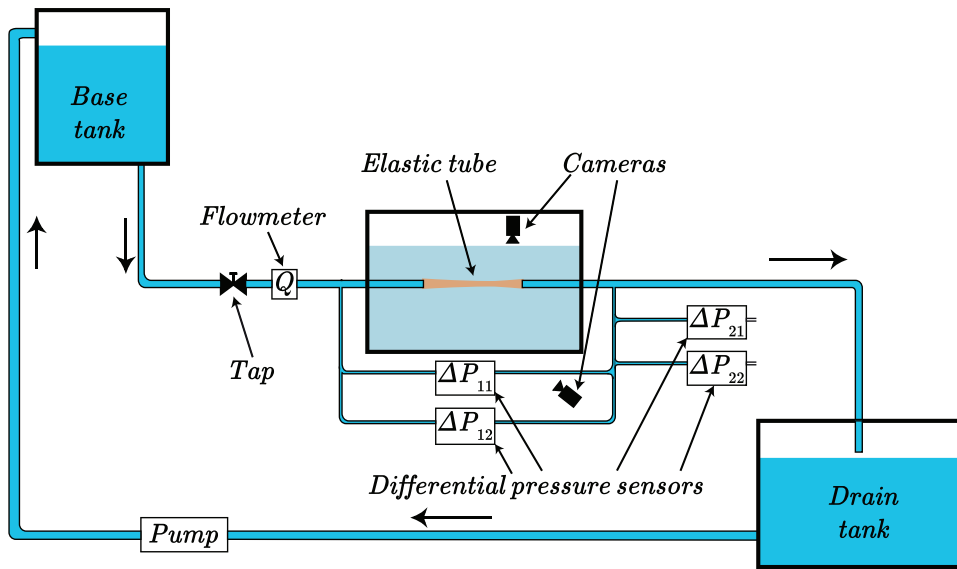


FIG. 2. Apparatus for investigations of stability and self-exciting oscillations of elastic tubes conveying fluid.

hose segments are much stiffer than the Penrose tube and can be considered rigid.

The working fluid flows in a closed circuit. The fluid is pumped into the base tank and sinks due to the action of gravity through the elastic tube. Next, the working fluid flows through the drain hose into the drain tank, closing the cycle. Since the base tank is located at a height of 12 m above the test section, the change in the fluid level in the base tank has a negligible effect on the flow rate  $Q$ , which is controlled by the tap. That is why unsteadiness caused by the pump operation does not affect the flow and measurements in the test section.

Given the pressure difference at the tap of the order of 1.2 atm (produced by the hydrostatic pressure of 12 m fluid column) and relatively small flow rates considered in this study, the tap was just slightly open so that it was effectively a reflection point for all perturbations coming out upstream from the collapsible segment. For perturbations moving downstream, the reflection point was at the open end of the drain hose.

### B. Measurement system

The average flow rate  $Q$  is measured by the ultrasonic flowmeter Karat 520 with relative measurement error 1%. The pressure drop  $\Delta p = p_1 - p_2$  (upstream pressure is  $p_1$  and downstream is  $p_2$ ) in the tube is changed by the flow rate  $Q$  or downstream pressure  $p_2$ . In its turn, the downstream pressure  $p_2$  is changed by the position of the drain hose. Two differential pressure sensors, BD sensors DMD 331 and Korund-DDN-001M, with working pressure ranges 100 and 10 kPa and measurement errors 500 and 100 Pa, respectively, record the instantaneous pressure drop between the inlet and outlet sections of the tube (one sensor was used for larger and the other for smaller pressure drops). Another pair of differential pressure sensors records the difference between outlet pressure  $p_2$  and atmospheric pressure  $p_a$ . The distance from the elastic tube to the pressure  $p_1$  sampling point is 0.5 m and to the pressure  $p_2$  sampling point is 0.3 m. Pressure sampling points and pressure gauges are connected by the tubes, and hence, only average values of pressure differences are measured

quantitatively correct, whereas instantaneous values (denoted hereunder by a prime:  $p'_1, p'_2$ ) are distorted by those tubes and retain only their qualitative properties, such as frequency and number of “aftershocks” after the collapse of the tube. Steady pressure drop in the rigid tube between each sampling point and the collapsible segment was subtracted from pressure gauge indications to get the pressure drop and outlet pressure right in the collapsible segment. Transmural pressure  $p_2 - p_e$  can be controlled either by  $p_2$  or by  $p_e$ . External pressure  $p_e$  can be changed by the level of water in the chamber; however, in all our tests, it was 0.09 m above the tubes, and  $p_e = p_a + 883$  Pa so that transmural pressure was changed by  $p_2$  only.

To visualize the oscillation modes of a tube, two cameras were used that were located above and on the side of the tube.

To verify the apparatus and the gauges operation, first, a section of a rigid tube was inserted instead of the elastic tube. All sensors have been calibrated on the apparatus with the rigid tube. The friction coefficients for different Reynolds numbers for the laminar and turbulent flow regimes were measured. Water was used as a working fluid in a turbulent regime and a glycerin solution of 33% mass concentration in a laminar regime. Good agreement between experimental data and classical theoretical curves (Fig. 3) was obtained in both regimes for the rigid tube case.

### C. Selection of the working fluid and operating mass flow range

As stated in Sec. I, the goal of this study is to isolate and to study the effect of the flow regime on the stability boundary and the tube oscillations. We organize two flows with the same flow rate: a turbulent flow of water and a laminar flow of the glycerin solution, which provide equal pressure differences  $p_1 - p_2$  and  $p_2 - p_e$ . Since we use identical tubes, these two flows are equivalent in terms of the flow rate, pressures, and tube shapes and differ in the flow regime inside of the tube. As seen from Fig. 1, this condition can be only met if a specific relationship between the flow rate and the viscosity of the glycerin

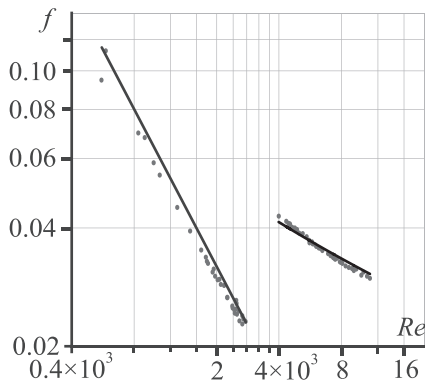


**FIG. 3.** Experimental data (points) of the flow friction coefficient  $f$  in the rigid tube as a function of Reynolds number for laminar and turbulent flows. Curves correspond to laminar  $64/Re$  and turbulent Blasius laws.

solution is fulfilled, i.e., for each flow rate we should utilize a different solution. This section establishes this relationship.

Let us denote the laminar flow by index “ $l$ ” and the turbulent flow by index “ $t$ .” Assume that the average velocities  $v_{av}$  and pressure drops  $\Delta p$  are the same for laminar and turbulent flows. We express the value of the pressure drop through the friction coefficient for pipe flow defined as

$$f = \frac{\Delta p}{L} \frac{D}{\rho v_{av}^2} \tag{1}$$

where  $D$  and  $L$  are the tube diameter and length.

To determine the turbulent friction coefficient in the elastic tube, a series of preliminary experiments was conducted for turbulent regimes. Water was used as a working fluid. The Reynolds number  $Re$  was within the range of 4000–8000. The experimental friction coefficient in the elastic tube is shown in Fig. 4 (points). The theoretical friction coefficient for a rigid tube shown in the same figure is calculated according to the empirical formulas of Blasius<sup>46</sup> and Filonenko,<sup>47</sup>

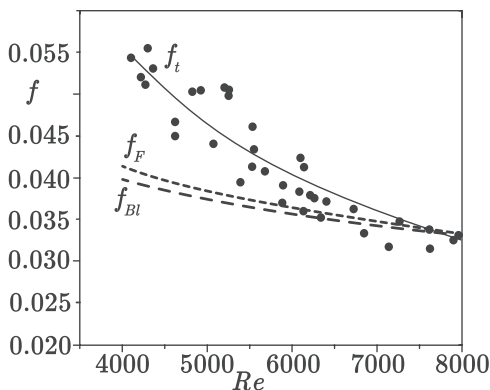


**FIG. 4.** Friction coefficient as a function of Reynolds number for turbulent flows. Curves  $f_{Bl}$  and  $f_F$  are the Blasius and Filonenko empirical formulas for a rigid tube, respectively;  $f_t$  is the approximation of the present experimental data for elastic tube.

$$f_{Bl} = \frac{0.3164}{Re^{0.25}}; \quad f_F = (1.82 \log(Re) - 1.64)^{-2} \tag{2}$$

It is seen that the friction coefficient for the case of the elastic tube is quite different from that for the rigid tube. This is consistent with the previously studied effect of elastic properties on the laminar-turbulent transition and friction coefficients: Verma and Kumaran<sup>48</sup> demonstrated that the change in transition (compared to rigid tubes) is not due to a slow change in the tube diameter, but associated with the wall elasticity. This was shown by fabricating a harder polydimethylsiloxane (PDMS) gel tube with the same shape as the soft deformable gel tube and demonstrating that the transition in the rigid gel tube is similar to that in a cylindrical tube. Later, Neelamegam and Shankar<sup>49</sup> demonstrated the effect of elasticity on deformable tubes made of polydimethylsiloxane gels of different shear moduli. In these studies, friction coefficient measured for turbulent flow in elastic tube was essentially larger than in a rigid tube, which is in accordance with our observations. In what follows, we use power law approximation  $f_t = 30.822/Re^{0.762}$  of our experimental data.

Equating the value for the pressure drop for turbulent and laminar flows, taking into account that the experimentally obtained friction coefficient for laminar flow in elastic tube is in reasonable correlation with the rigid tube case,  $f_l = 64/Re$  (Fig. 5), and expressing the average speed in terms of the flow rate, we obtain

$$Q = \frac{\pi D}{4} \left( \frac{64 \nu_l \rho_l}{30.822 \rho_t \nu_t^{0.762}} \right)^{\frac{1}{0.238}} \tag{3}$$

Given that the viscosity and density of the glycerin solution at a temperature of 20 °C are known functions of the concentration, formula (3) determines the required viscosity (concentration) of the glycerin hydrous solution for each flow rate thus ensuring that the pressure drop is the same as in the corresponding turbulent flow of water.

It is also necessary that the flow rate (3) corresponds to turbulent range of Reynolds numbers for the case of water and to laminar range for the case of glycerin solution, i.e.,

$$Q_t < Q < Q_l \tag{4}$$

The flow rate function has the form

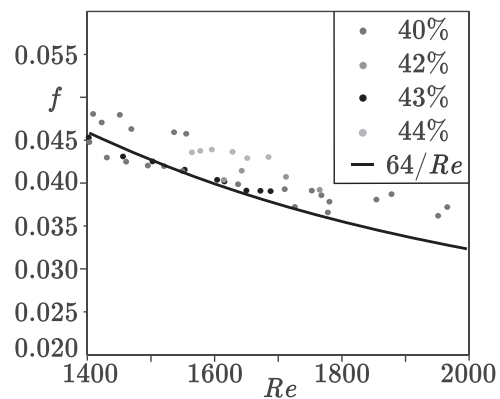


**FIG. 5.** Friction coefficient as a function of Reynolds number for laminar fluid flows with different viscosity in elastic tube.

$$Q_{l,t} = \frac{Re_{l,t} \nu_{l,t} \pi D}{4},$$

where the value  $Re_t = 4000$  was taken as minimum Reynolds number that guarantees developed turbulent regimes and  $Re_l = 1800$  was taken as maximum Reynolds number that guarantees laminar flow. Flow rate (3) vs the concentration of glycerin solution is shown in Fig. 6. We find that the flow rate range from 1.9 to 3.2 l/min and the mass concentration of glycerin hydrous solution from 40% to 44% at a temperature of 20 °C are the necessary conditions for the equivalence of laminar and turbulent flow that is met in our experiments.

To guarantee constant fluid properties during each test, the temperature and viscosity of glycerin hydrous solution were checked before, during, and after the experiments with each solution. It was found that the characteristics of the solution changed insignificantly during the experiments. Moreover, when switching to the next fluid, at least 4 full recirculation cycles (complete transfer of the fluid from the drain tank to the base tank and flow back through the tube) were run to fully mix the solution and secure its properties.

#### D. Measure of equivalence of the laminar and turbulent flow

As seen from the previous subsection, the equivalence between laminar and turbulent flows takes place, for each glycerin solution, only for one certain value of the flow rate. For any other flow rate, flow regimes are not exactly equivalent, because their friction coefficients obey different laws. Hence, the problem analyzed in this study—isolation of the flow regime effect—in the general sense is not solvable in principle: there are no fluids that will be equivalent in a range of flow rates or pressure differences and correspond to different flow regimes (one to laminar and the other to turbulent). That is why we should choose a certain flow rate and certain pressure differences, for which the flows will be equivalent. Given that friction coefficients can be firmly established only for a steady flow in a circular tube, it is natural to choose these parameters in the stable state of the tube, but close to the stability boundary. In this case, we have two flows, one of which loses stability close to the equivalence point, but the other stays stable longer, which fulfills the goal of this study in the sense of stability boundary.

However, for postcritical oscillation regimes, the exact equivalence does not exist *a priori*. When comparing them, we assume

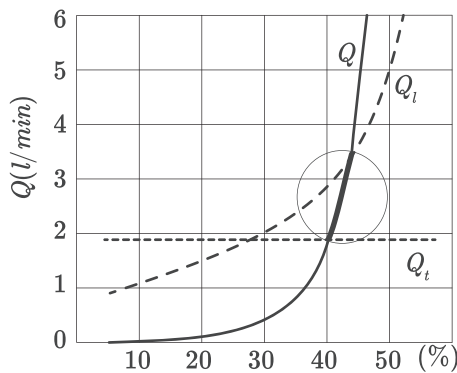


FIG. 6. Flow rate (3) as a function of the glycerin hydrous solution concentration; segment satisfying (4) is shown in bold.

equivalence not in the sense of friction coefficients, but in the sense of two “equivalent” dynamical systems. Namely, we have two collapsible tubes that differ at a certain flow rate and pressure drop (where the tubes are stable) only by the flow regime. Assuming the equivalence at this certain point to be an equivalence of the dynamical systems, we then compare and analyze their postcritical behavior at other flow rates and pressure drops. Surprisingly, as will be shown below, postcritical oscillation modes at laminar and turbulent flows correspond to close pressure drops, which is an unexpected experimental result. This is why we can consider these regimes as *approximately* equivalent.

#### E. Tube diameter

Since the tube made of elastic material is used in the experiments, its diameter varies depending on the transmural pressure. A series of experiments was done to determine the elastic tube diameter for different values of the outlet pressure. The diameter was measured by a hand caliper. Measures were taken near the inlet, middle, and outlet sections, and in all cases, the diameter was nearly constant. This means that the tube constriction due to viscous loss was negligible for the considered range of flow rates. Experimental points with RMS deviation 0.000 19 m due to different samples of elastic tubes and due to measurement errors under various flow conditions were approximated by a linear relation  $D = 2 \times 10^{-7}(p_2 - p_e) + 0.0094$  (Fig. 7).

### III. RESULTS

#### A. Typical oscillation regimes

When the average pressure drop  $\Delta p = p_1 - p_2$  is increased while maintaining a constant flow rate  $Q$ , the stability is lost by passing through a certain critical value  $\Delta p_{cr}$  and the tube starts to oscillate. Static instability preceding flutter was either not detected, or (for small flow rates) had a negligible range of pressure drops so that it can be neglected in further considerations. The observed oscillation mode is unique for each mean pressure drop and flow rate, no matter if the regime was obtained by increasing or decreasing the mean pressure drop or flow rate, and without any reaction to manual perturbations of the tube.

Four modes of oscillations were identified in experiments; resulting plots of instantaneous pressure drops  $\Delta p'$  are shown in Figs. 8(a)–8(d). One pronounced peak is present in all modes of oscillations and it corresponds to a sharp increase and following decrease in the pressure drop

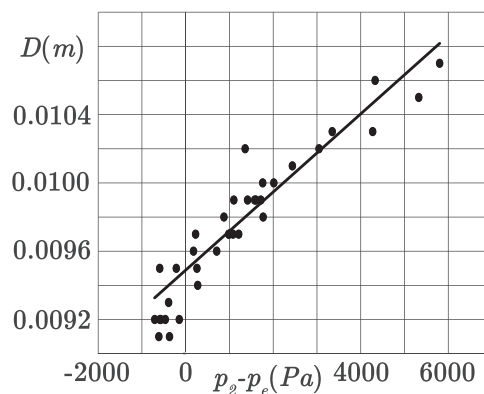


FIG. 7. Tube diameter as a function of transmural pressure.

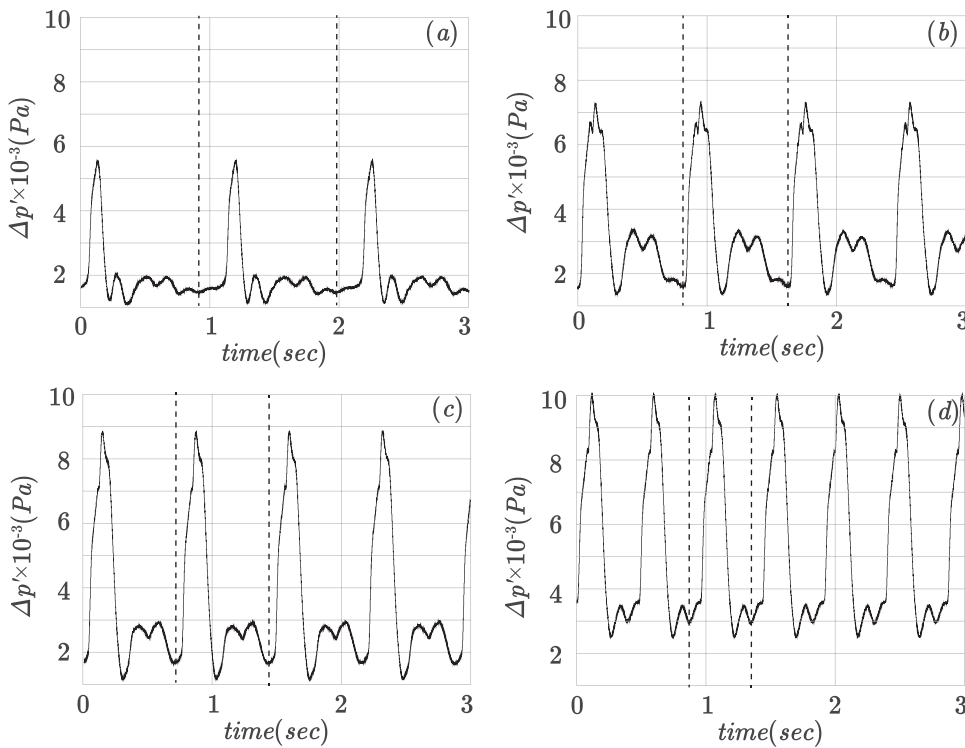


FIG. 8. Four oscillation modes observed by differential pressure readings: the fourth (a), the third (b), the second (c), and the first (d) mode. Dotted lines show a single oscillation period.

associated with the primary collapse of the tube. After this dominant peak, there are four, three, two, or one small peak in the pressure drop for the fourth [Fig. 8(a)], third [Fig. 8(b)], second [Fig. 8(c)], and first [Fig. 8(d)] mode of oscillation, respectively.

**B. Instability of the elastic tube with turbulent flow inside**

First, experiments are conducted at the turbulent flow regime for the flow rate  $Q$  from 2.2 to 4 l/min with a step of 0.2 l/min; water is used as the working fluid. The downstream pressure  $p_2$  is changed by the positioning of the drain hose outlet, whereas the upstream pressure  $p_1$  remains almost unchanged at the fixed flow rate. In result, the average pressure drop gradually rises until the onset of oscillation, i.e., loss of stability; next, a sharp jump in average pressure drop occurs and oscillations in the form of the third mode begin. With a further increase in the average pressure drop, the regions of the oscillation modes previously identified in Sec. III A are observed: the third mode is followed by the second, and then, for a larger average pressure drop, by the first mode.

Regions of oscillation modes described above are shown in Fig. 9. Alternatively, the range of vibration modes can also be distinguished by the transmural pressure  $p_2 - p_e$  plotted vs the flow rate, Fig. 10, with the exception of the stability and oscillations in the third mode that occupy the same range of transmural pressures.

**C. Instability of the elastic tube with laminar flow inside**

Experiments in the case of a laminar flow regime are conducted similarly as in the case of a turbulent regime; the emphasis is made on

identifying the effect of viscosity. Water solutions of glycerin with a percentage of 42%, 43%, and 44% are used as the working fluid, and the flow rate varies from 2.3 to 2.7 l/min.

After the loss of stability, a small jump in the average pressure drop occurs and oscillations in the form of the fourth mode start. After the next jump in average pressure drop, the oscillations are switched to the third mode with a further increase in average pressure drop. Then oscillations pass to the second mode, and then to the first mode with successive increases in the average pressure drop.

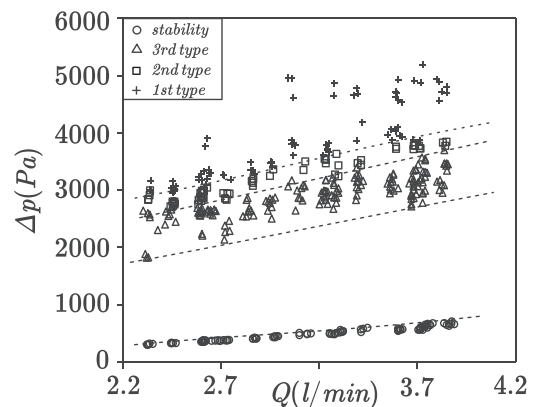


FIG. 9. Average pressure drop as a function of flow rate for turbulent flow; dashed lines roughly separate different oscillation modes.

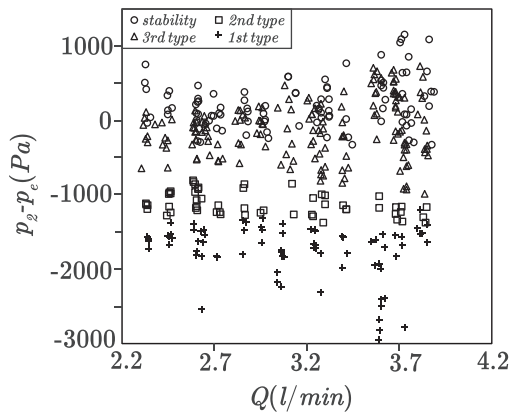


FIG. 10. Average transmural pressure as a function of flow rate for turbulent flow.

The division into regions by oscillation modes is shown in Fig. 11. It is seen that a small change in viscosity does not affect the transition boundary between the oscillation modes.

As well as for turbulent flow, the ranges of oscillation modes can also be distinguished by the transmural pressure  $p_2 - p_e$  plotted vs the flow rate, Fig. 12. However, it is hard to separate the region of stability and the fourth oscillation mode by  $p_2 - p_e$  measurements only. Note that the fourth mode of oscillation is typical only for laminar flows and is not observed in turbulent flows. Moreover, it is seen that in terms of average pressure drop  $\Delta p$ , the transition from stability to the oscillations occurs smoother in the laminar flow due to the appearance of the fourth mode of oscillation.

D. Comparison of laminar and turbulent flows

Figure 13 shows detailed comparison of stability boundaries at laminar and turbulent regimes (error bars are associated with uncertainties of the pressure gauge and flow meter). It is seen that the stability loss in the turbulent flow regime occurs at a lower average pressure drop than in the laminar flow, i.e., the laminar flow is more stable. According to the map of oscillation modes shown in Fig. 14, after the loss of stability, there is a sharp increase in the average pressure drop

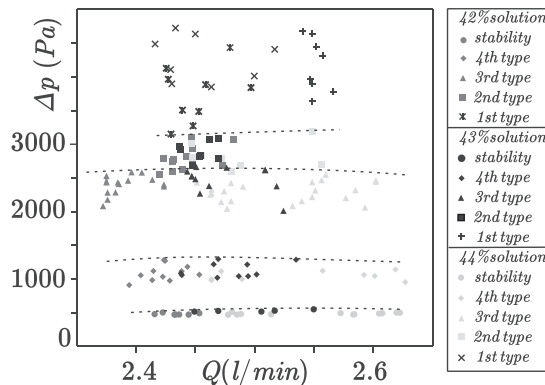


FIG. 11. Average pressure drop as a function of flow rate for laminar flows; dashed lines roughly separate different oscillation modes.

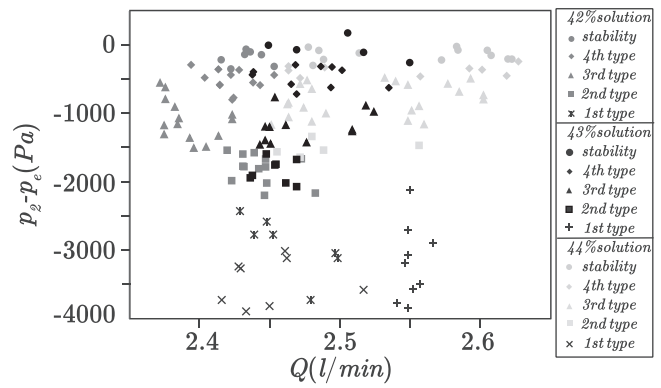


FIG. 12. Average transmural pressure as a function of flow rate for laminar flows.

in the turbulent regime, and oscillations of the third mode are observed. At the same time, the oscillations of the elastic tube with laminar flow inside occur in the fourth mode and only with a further increase in average pressure drop, move to the third mode.

The third oscillation mode takes place at roughly the same average pressure drops in both regimes. The oscillations move to the second mode with a further increase in the average pressure drop, and the transition from the third to the second mode occurs at almost the same average pressure drops for turbulent and laminar flows. However, the difference in the transition to the first mode is more pronounced: at turbulent regimes, it occurs at a lower average pressure drop than at the laminar regime.

Let us now compare the oscillation frequencies for the laminar and turbulent flows. The frequency spectrum of each measured time sample was processed and a dominant frequency (related to the period of oscillations) was extracted. The resulting values were extrapolated to make the frequency color map shown in Figs. 15 and 16. The tube oscillates with a frequency in the range of 0.9–1.4, 1.35–1.5, 1.4–1.95 Hz (Fig. 15), at the third, second, and first modes, respectively, for the turbulent flow. For the same modes at laminar flow, the frequency ranges are 1.0–1.25, 1.25–1.50, 1.5–2.50 Hz (Fig. 16). For the fourth mode that exists only at the laminar flow, the frequency range is 0.5–1.0 Hz. Hence, in the laminar flow, the frequency increase due to the increase in the average pressure drop  $\Delta p$  is more significant than in the turbulent flow.

Finally, consider the amplitude of oscillations. Based on the pressure drop shown in Fig. 17 (and similar measurements), we conclude that the oscillation amplitude for a turbulent flow is higher than for a

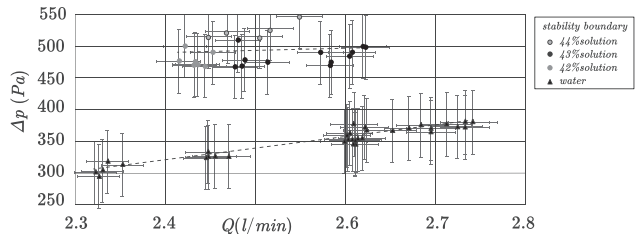


FIG. 13. Average pressure drop as a function of flow rate at the stability boundary; trend lines are shown by dashed lines.

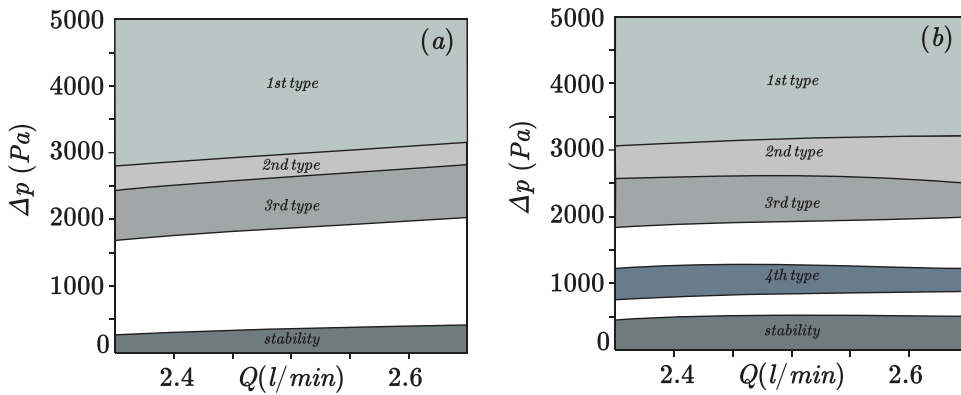


FIG. 14. Average pressure drop as a function of flow rate for turbulent (a), laminar (b) flow and corresponding maps of the regimes.

laminar flow for all oscillation modes. Recall that although the transient signal can be distorted by tubes connecting pressure sampling points and pressure gauges, qualitative relations remain unchanged. Larger amplitude at turbulent regimes implies higher degree of the tube collapse; this will be confirmed below by the tube visualization. It is interesting to note this difference in the oscillation amplitude even for quite close average pressure drops. Consequently, even for the observed *approximate* equivalence of the oscillation modes in the sense of average pressure drop (although *exact* equivalence is not possible, as was mentioned in Sec. IID), the peak amplitude and, hence, oscillation modes, are different.

**E. Visualization of instability modes for laminar and turbulent flow**

Synchronous video recording of the top and side views was conducted by two cameras indicated in Fig. 2 to compare the vibration modes of the elastic tube.

Observation of top-view pictures [Figs. 18(b), 18(d), 19(b), 19(d), 20(b), and 20(d)] shows that the tube cross section in the collapsed state has a shape of a dumbbell. The maximum tube compression during an oscillation cycle increases with a sequential transition from the third oscillation mode to the second and reaches maximum collapse at the first mode in both turbulent and laminar regimes. It is seen that the collapsed segment is longer and smoother in the laminar regime

(Figs. 18(c), 18(d), 19(c), 19(d), 20(c), and 20(d)) and it is shorter and sharper in the turbulent regime (Figs. 18(a), 18(b), 19(a), 19(b), 20(a), and 20(b)) for all oscillation modes. Hence, the tube is more collapsed at the turbulent regime, which is in consistency with the higher amplitude of pressure waves discussed above.

**IV. DISCUSSION**

As a result of experimental observations, two conclusions can be made as follows:

1. For the case of laminar flows, the instability occurs for larger pressure drops, i.e., laminar steady flow in collapsible tube is more stable than turbulent.
2. After the loss of stability, the amplitude of oscillations is larger for the turbulent flows than for the laminar; also, the second and subsequent pressure peaks in each cycle of oscillations are more pronounced for the turbulent flows.

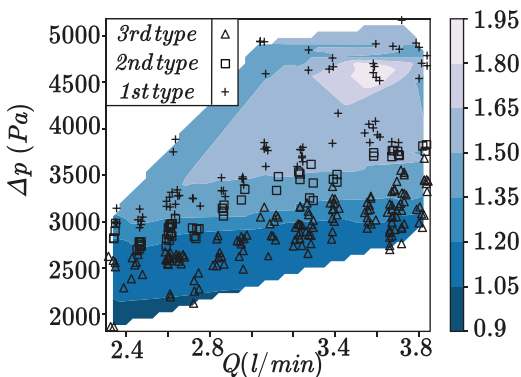
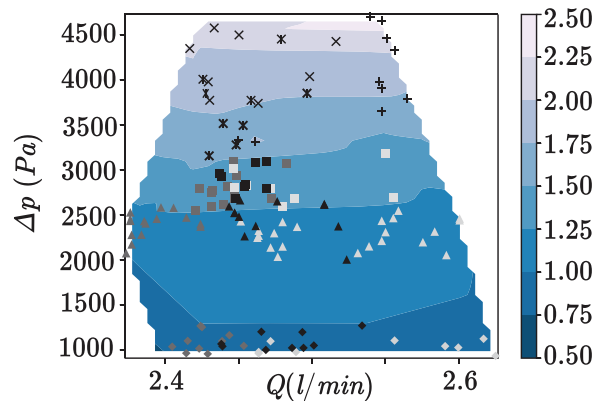


FIG. 15. The oscillation frequencies for the turbulent (a) flows. Color map corresponds to dominant frequency (Hz).



	42% solution	43% solution	44% solution
4th type	♦	♦	♦
3rd type	▲	▲	▲
2nd type	■	■	■
1st type	+	*	×

FIG. 16. The oscillation frequencies for laminar flows. Color map corresponds to dominant frequency (Hz).

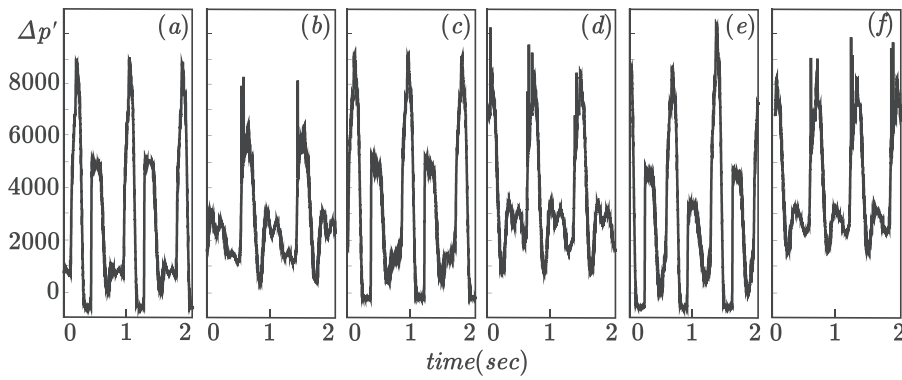


FIG. 17. Instantaneous pressure drop as a function of time for oscillations in the third, second, and first modes for turbulent (a), (c), and (e) and laminar (b), (d), and (f) flow.

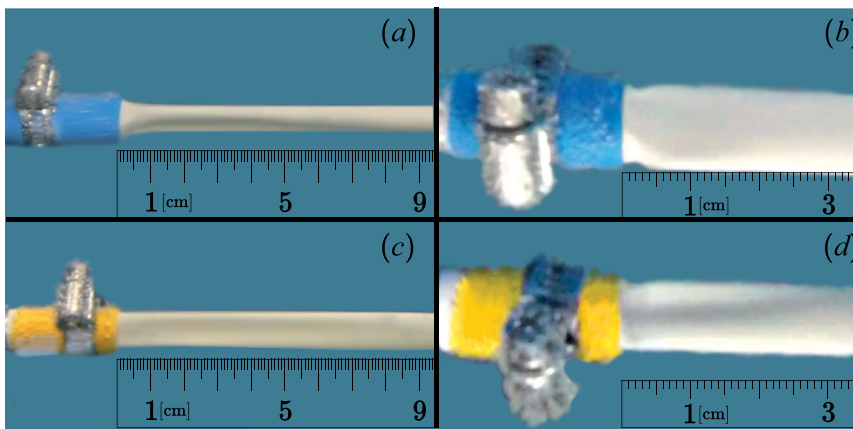


FIG. 18. Instantaneous tube deformation during the third oscillation mode for (a) turbulent flow, side view, (b) turbulent flow, top view, (c) laminar flow, side view, (d) laminar flow, top view.

The first conclusion can be explained theoretically. First, consider a laminar, more stable than turbulent, flow at its stable state (round tube, steady Poiseuille flow). The stability is lost when small deviations of the tube diameter yield the pressure deviation that cannot be sustained by the tube, which then loses axisymmetry, collapses, and the flow detaches from the tube walls. The conditions for the instability are more favorable, when the pressure decrease caused by a small decrease in the diameter is larger, i.e., for larger value of  $dp/dD$ . Taken

into account that the inlet pressure and the diameter are given by the upstream rigid segment of the tube, this condition can be reformulated as follows: the instability will onset earlier for larger value of  $d(\text{grad}p)/dD$ , where  $\text{grad}p = \Delta p/L$  is the pressure gradient (positive gradient corresponds to the pressure decrease downstream). Let us now calculate this derivative for laminar and turbulent flows.

Consider three steady flows: laminar flow, turbulent flow in the rigid tube, and turbulent flow in the elastic tube (recall that laminar

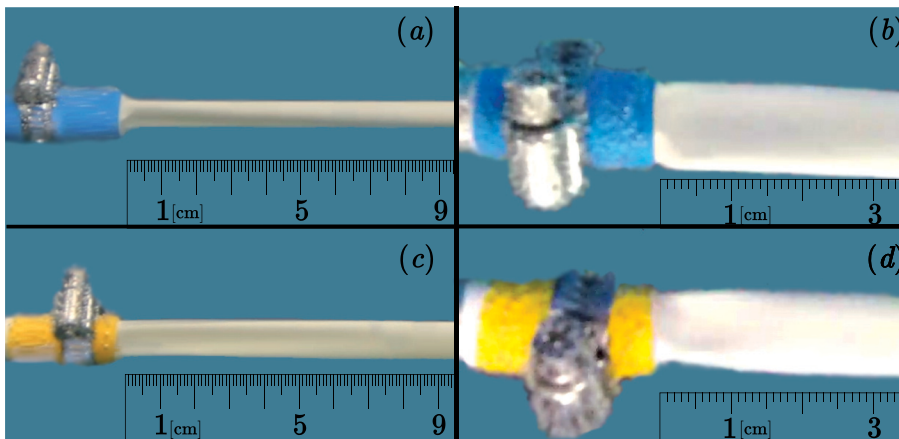


FIG. 19. Tube deformation during the second oscillation mode for (a) turbulent flow, side view, (b) turbulent flow, top view, (c) laminar flow, side view, (d) laminar flow, top view.

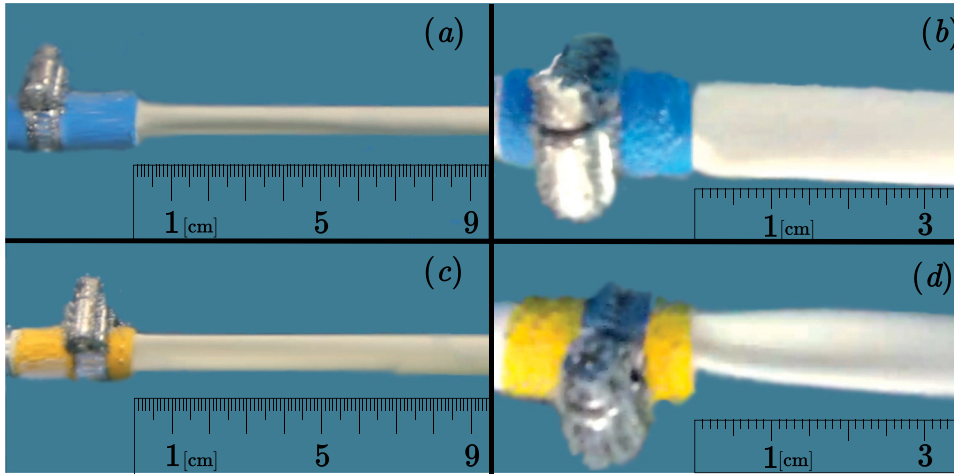


FIG. 20. Tube deformation during the first oscillation mode for (a) turbulent flow, side view, (b) turbulent flow, top view, (c) laminar flow, side view, (d) laminar flow, top view.

flow in rigid and elastic tubes has the same friction coefficient  $f = 64/Re$ , which corresponds to the same flow rate, pressure gradient, and tube diameter. For the local pressure gradient, we have

$$\text{grad}p(D) = f(Re) \frac{\rho v^2}{2D}, \quad Re = Re(D) = \frac{v(D)D}{\nu},$$

$$v = v(D) = \frac{4Q}{\pi D^2},$$

and friction coefficient for laminar flow ( $l$ ), turbulent flow in the rigid tube ( $Bl$ ), and turbulent flow in the elastic tube ( $t$ ) are (Sec. II B)

$$f_l(Re) = \frac{64}{Re}, \quad f_{Bl}(Re) = \frac{0.3164}{Re^{0.25}}, \quad f_t(Re) = \frac{30.822}{Re^{0.762}}.$$

Consider a small deviation of the tube diameter in the collapsible segment for the unchanged flow rate  $Q$ . By direct calculation, we find

$$\left. \frac{d(\text{grad}p)}{dD} \right|_l = -4 \frac{\rho_l v^2}{2} \frac{f_l}{D^2}, \quad \left. \frac{d(\text{grad}p)}{dD} \right|_{Bl} = -\frac{19}{4} \frac{\rho_l v^2}{2} \frac{f_{Bl}}{D^2},$$

$$\left. \frac{d(\text{grad}p)}{dD} \right|_t = -4.238 \frac{\rho_t v^2}{2} \frac{f_t}{D^2}.$$

Due to the equal steady pressure drop,  $\rho_l f_l = \rho_t f_{Bl} = \rho_t f_t$ ; consequently,

$$\left. \frac{d(\text{grad}p)}{dD} \right|_l = \frac{16}{19} \left. \frac{d(\text{grad}p)}{dD} \right|_{Bl}, \quad (5)$$

$$\left. \frac{d(\text{grad}p)}{dD} \right|_l = 0.944 \left. \frac{d(\text{grad}p)}{dD} \right|_t,$$

which means that small decrease in the tube diameter yields smaller pressure decrease for laminar, rather than for turbulent flow, both for rigid and elastic tube. Therefore, laminar flow is more stable, which is fully confirmed by experimental observations.

It is well known that in experimental studies of collapsible tubes, the oscillations are driven not only by the collapsible segment but also by the apparatus itself, because flow perturbations move both upstream (and reflect from the tap) and downstream (and reflect from the drain hose outlet); also, partial reflections are possible from points of the diameter change. The natural question is whether our

conclusions are apparatus-dependent? It is clear that the conclusion 1 is not: the stability boundary itself is not related to oscillations formed after the loss of stability, and the simple theoretical explanation given above does not involve the apparatus. More care is needed for the conclusion 2. We expect that the difference in oscillation amplitudes (which are larger at turbulent flow conditions) does not depend on the apparatus, because the dominant collapse (loss of the stability by the tube and flow detachment) occurs extremely fast—much faster than any perturbation can reach any reflection point; hence, the peak amplitude is governed by the collapsed segment and not by the apparatus. Consequently, the two principal conclusions obtained in this study are rather general.

What the apparatus partially drives is the oscillation frequencies and sequence of oscillation modes, because each cycle of oscillations involves reflections of perturbations from the tap and outlet of the drain hose. However, the difference between oscillation frequency at laminar and turbulent flows demonstrated at our apparatus will in general retain at a different setup. Hence, we can reformulate this frequency-related conclusion in a “weak,” apparatus-independent form: frequency oscillations and oscillation modes are different for laminar and turbulent flows.

### V. CONCLUSIONS

In this study, we compared the stability boundary and oscillation modes of collapsible tubes conveying fluids at laminar and turbulent regimes at the conditions of equal average flow rate, pressure drop, transmural pressure, and steady tube geometry. Theoretical considerations show that in order to obtain laminar regimes equivalent to turbulent flows of water, a flow rate between 1.9 and 3.2 l/min and a concentration of the water glycerin solutions from 40% to 44% at a temperature of 20 °C are necessary for equal integral characteristics.

Equivalent stability experiments were done separately for water (turbulent) and water glycerin solution (laminar) flows. After the loss of stability, we identified four oscillation modes, which correspond, at each oscillation cycle, to one strong peak of the pressure drop, followed by one, two, three, or four additional peaks of smaller amplitude.

It was found that the stability loss of the steady turbulent flow regime occurs at a lower pressure drop than in the steady laminar flow; this result was explained theoretically and does not depend on

the particular apparatus used in this study. When crossing the stability boundary at the turbulent regime, the third oscillation mode is realized accompanied by a sharp increase in the average pressure drop. After crossing the stability boundary at the laminar regime, oscillations occur in the fourth mode and switch to the third mode with a further increase in the average pressure drop. The average pressure drops at the third oscillation mode and the boundary between the third and second modes for turbulent and laminar flows are close. However, with a further increase in the average pressure drop, the transition to the first mode at the turbulent regime occurs at a lower average pressure drop than for the laminar. Although the sequence of oscillation modes is valid, strictly speaking, only at our particular apparatus, the difference in the sequence, as well as in oscillation frequency, between laminar and turbulent flows, may occur at a different setup. We have also observed that the amplitude of oscillations is larger at turbulent regimes; given that the amplitude (which reflects the degree of the tube collapse) is driven only by the collapsible segment, we expect that this result will be valid at any collapsible-tube setup.

The results of this study show that the stability boundary and oscillation modes of collapsible tube conveying fluid are different for laminar and turbulent regimes, even if their integral parameters (flow rate, pressure drop, transmural pressure, tube shape) are close. Hence, experimental studies, which are often conducted at turbulent flow conditions, and numerical models validated at turbulent regimes should be applied to laminar physiological flows with care. Also, the flow limitation caused by the collapses of the blood vessel can be different depending on the flow regime, which can result in a difference of blood flow circulation. Such biomechanical applications, hence, need special experiments, where both the flow regime and (if non-Newtonian) rheology of the fluid should be accurately reproduced.

## ACKNOWLEDGMENTS

The authors are grateful to Oleg O. Ivanov, Vladimir V. Trifonov, and Alexander I. Reshmin for their help with arranging the experimental apparatus and numerous discussions of the problem.

The work is supported by RFBR Grant Nos. 18–29–10020 and 20–31–90018.

## DATA AVAILABILITY

The data that support the findings of this study are available within the article.

## REFERENCES

- <sup>1</sup>A. Shapiro, “Physiological and medical aspects of flow in collapsible tubes,” in Proceedings of the 6th Canadian Congress on Applied Mathematics (1977), pp. 883–906.
- <sup>2</sup>A. Shapiro, “Steady flow in collapsible tubes,” *ASME J. Biomech. Eng.* **99**, 126–147 (1977).
- <sup>3</sup>R. Kamm and A. Shapiro, “Unsteady flow in a collapsible tube subjected to external pressure or body forces,” *J. Fluid Mech.* **95**, 1–78 (1979).
- <sup>4</sup>T. Pedley, “Wave phenomena in physiological flows,” *IMA J. Appl. Math.* **32**, 267–287 (1984).
- <sup>5</sup>T. Pedley, B. Brook, and R. Seymour, “Blood pressure and flow rate in the giraffe jugular vein,” *Philos. Trans. R. Soc. London B* **351**, 855–866 (1996).
- <sup>6</sup>V. Koshev, E. Petrov, and A. Volobuev, *A Hydrodynamic Flutter and Antiflutter Stabilization in The Cardiovascular System—A Hydrodynamic Pattern and General Theory of Circulation* (Ofort, 2007) (in Russian).
- <sup>7</sup>J. Grotberg and O. Jensen, “Biofluid mechanics in flexible tubes,” *Ann. Rev. Fluid Mech.* **36**, 121–147 (2004).
- <sup>8</sup>C. Bertram, “Experimental studies of collapsible tubes,” in *Flow Past Highly Compliant Boundaries and in Collapsible Tubes* (Kluwer, 2003), pp. 51–65.
- <sup>9</sup>M. Heil and A. Hazel, “Fluid-structure interaction in internal physiological flows,” *Ann. Rev. Fluid Mech.* **43**, 141–162 (2011).
- <sup>10</sup>L. Formaggia, D. Lamponi, and A. Quarteroni, “One-dimensional models for blood flow in arteries,” *J. Eng. Math.* **47**, 215–276 (2003).
- <sup>11</sup>J. Alastruey, S. Moore, K. Parker, T. David, J. Peiro, and S. Sherwin, “Reduced modelling of blood flow in the cerebral circulation: Coupling 1-D, 0-D and cerebral auto-regulation models,” *Int. J. Numer. Methods Fluids* **56**, 1061–1067 (2008).
- <sup>12</sup>P. Reymond, F. Merenda, F. Perren, D. Rufenacht, and N. Stergiopoulos, “Validation of a one-dimensional model of the systemic arterial tree,” *Am. J. Physiol.: Heart Circ. Physiol.* **297**, H208–H222 (2009).
- <sup>13</sup>J. Alastruey, A. Khir, K. Matthys, P. Segers, S. Sherwin, R. Verdonck, K. Parker, and J. Peiro, “Pulse wave propagation in a model human arterial network: Assessment of 1-D visco-elastic simulations against *in vitro* measurements,” *J. Biomech.* **44**, 2250–2258 (2011).
- <sup>14</sup>Y. V. Vassilevski, V. Salamatova, and S. S. Simakov, “On the elasticity of blood vessels in one-dimensional problems of hemodynamics,” *Comput. Math. Math. Phys.* **55**, 1567–1578 (2015).
- <sup>15</sup>P. Blanco, S. Watanabe, M. Passos, P. Lemos, and R. Feijoo, “An anatomically detailed arterial network model for one-dimensional computational hemodynamics,” *IEEE Trans Biomed. Eng.* **62**, 736–753 (2015).
- <sup>16</sup>D. Guan, F. Liang, and P. Gremaud, “Comparison of the Windkessel model and structured-tree model applied to prescribe outflow boundary conditions for a one-dimensional arterial tree model,” *J. Biomech.* **49**, 1583–1592 (2016).
- <sup>17</sup>A. Poroshina and V. Vedenev, “Existence and uniqueness of the stationary state of elastic tubes conveying power law fluid,” *Russ. J. Biomech.* **22**, 169–193 (2018).
- <sup>18</sup>V. Vedenev, “Nonlinear steady states of hyperelastic membrane tubes conveying a viscous non-Newtonian fluid,” *J. Fluids Struct.* **98**, 103113 (2020).
- <sup>19</sup>A. Il'ichev, “Dynamics and spectral stability of soliton-like structures in fluid filled membrane tubes,” *Russ. Math. Surv.* **75**(5), 843–882 (2020).
- <sup>20</sup>R. Whittaker, M. Heil, O. Jensen, and S. Waters, “Predicting the onset of high-frequency self-excited oscillations in elastic-walled tubes,” *Proc. R. Soc. A* **466**, 3635–3657 (2010).
- <sup>21</sup>V. Vedenev and A. Poroshina, “Stability of an elastic tube conveying a non-Newtonian fluid and having a locally weakened section,” *Proc. Steklov Inst. Math.* **300**, 34–55 (2018).
- <sup>22</sup>T. Pedley and X. Luo, “Modelling flow and oscillations in collapsible tubes,” *Theor. Comput. Fluid Dyn.* **10**, 277–294 (1998).
- <sup>23</sup>X. Luo and T. Pedley, “Multiple solutions and flow limitation in collapsible channel flows,” *J. Fluid Mech.* **420**, 301–324 (2000).
- <sup>24</sup>R. Kudenatti, N. Bujurke, and T. Pedley, “Stability of two-dimensional collapsible-channel flow at high Reynolds number,” *J. Fluid Mech.* **705**, 371–386 (2012).
- <sup>25</sup>H. Liu, X. Luo, and Z. Cai, “Stability and energy budget of pressure-driven collapsible channel flows,” *J. Fluid Mech.* **705**, 348–370 (2012).
- <sup>26</sup>M. Amaouche and G. D. Labbio, “Linear and weakly nonlinear global instability of a fluid flow through a collapsible channel,” *Phys. Fluids* **28**, 044106 (2016).
- <sup>27</sup>M. Heil and T. Pedley, “Large post-buckling deformations of cylindrical shells conveying viscous flow,” *J. Fluids Struct.* **10**, 565–599 (1996).
- <sup>28</sup>A. Hazel and M. Heil, “Steady finite-Reynolds-number flows in three-dimensional collapsible tubes,” *J. Fluid Mech.* **486**, 79–103 (2003).
- <sup>29</sup>A. Marzo, X. Luo, and C. Bertram, “Three-dimensional collapse and steady flow in thick-walled flexible tubes,” *J. Fluids Struct.* **20**, 817–835 (2005).
- <sup>30</sup>M. Heil and J. Boyle, “Self-excited oscillations in three-dimensional collapsible tubes: Simulating their onset and large-amplitude oscillations,” *J. Fluid Mech.* **652**, 405–426 (2010).
- <sup>31</sup>F. Knowlton and E. Starling, “Unsteady flow in a collapsible tube subjected to external pressure or body forces the influence of variations in temperature and blood pressure on the performance of the isolated mammalian heart,” *J. Physiol.* **44**, 206–219 (1912).

- <sup>32</sup>C. Bertram, C. Raymond, and T. Pedley, "Mapping of instabilities for flow through collapsed tubes of different length," *J. Fluids Struct.* **4**, 125–153 (1990).
- <sup>33</sup>J. Grotberg, "Respiratory fluid mechanics," *Phys. Fluids* **23**, 021301 (2011).
- <sup>34</sup>M. Amabili, P. Balasubramanian, I. Bozzo, I. Breslavsky, G. Ferrari, G. Franchini, G. Giovannello, and C. Pogue, "Nonlinear dynamics of human aortas for material characterization," *Phys. Rev. X* **10**, 011015 (2020).
- <sup>35</sup>N. Gavriely, T. Shee, D. Cugell, and J. Grotberg, "Flutter in flow-limited collapsible tubes: A mechanism for generation of wheezes," *J. Appl. Physiol.* **66**, 2251–2261 (1989).
- <sup>36</sup>R. Brower and A. Noordergraaf, "Pressure-flow characteristics of collapsible tubes: A reconciliation of seemingly contradictory results," *Ann. Biomed.* **1**, 333–355 (1973).
- <sup>37</sup>C. Bertram and R. Castles, "Flow limitation in uniform thick-walled collapsible tubes," *J. Fluids Struct.* **13**, 399–418 (1999).
- <sup>38</sup>C. Bertram and N. Elliott, "Flow-rate limitation in a uniform thin-walled collapsible tube, with comparison to a uniform thick-walled tube and a tube of tapering thickness," *J. Fluids Struct.* **17**, 541–559 (2003).
- <sup>39</sup>R.-Q. Wang, T. Lin, P. Shamsbery, G. Amos, and V. Winter, "Control of flow limitation in flexible tubes," *J. Mech. Des.* **139**, 013401 (2017).
- <sup>40</sup>C. Lyon, J. Scott, and C. Wang, "Flow through collapsible tubes at low Reynolds numbers. applicability of the waterfall model," *Circ. Res.* **47**, 68–73 (1980).
- <sup>41</sup>J. Duomarco and R. Rimini, "Energy and hydraulic gradient along systemic veins," *Am. J. Physiol.* **178**, 215–219 (1954).
- <sup>42</sup>R. Lopez-Muniz, N. Stephens, B. Bromberger-Barnea, S. Pemutt, and R. Riley, "Critical closure of pulmonary vessels analyzed in terms of starling resistor model," *J. Appl. Physiol.* **24**, 625–635 (1968).
- <sup>43</sup>C. Bertram and J. Tscherry, "The onset of flow-rate limitation and flow-induced oscillations in collapsible tubes," *J. Fluids Struct.* **22**, 1029–1045 (2006).
- <sup>44</sup>J. Zayko and V. Vedenev, "Self-exciting oscillations of elastic tube conveying fluid at laminar and turbulent flow regimes," *J. Phys.: Conf. Ser.* **894**, 012030 (2017).
- <sup>45</sup>S. Nahar, B. N. Dubey, and E. J. Windhab, "Influence of flowing fluid property through an elastic tube on various deformations along the tube length," *Phys. Fluids* **31**, 101905 (2019).
- <sup>46</sup>H. Schlichting, *Boundary-Layer Theory* (McGraw-Hill, 1979), p. 817.
- <sup>47</sup>G. Filonenko, "Hydraulic resistance of pipelines," *Therm. Eng.* **4**, 40–44 (1954) (in Russian).
- <sup>48</sup>M. Verma and V. Kumaran, "A dynamical instability due to fluid-wall coupling lowers the transition Reynolds number in the flow through a flexible tube," *J. Fluid Mech.* **705**, 322–347 (2012).
- <sup>49</sup>R. Neelamegam and V. Shankar, "Experimental study of the instability of laminar flow in a tube with deformable walls," *Phys. Fluids* **27**, 024102 (2015).